JOURNAL OF GEOPHYSICAL RESEARCH, VOL. 103, NO. D8, PAGES 8795–8803, APRIL 27, 1998

# Apparent breakdown of reciprocity in reflected solar radiances

Larry Di Girolamo, Tamás Várnai, and Roger Davies
Institute of Atmospheric Physics, The University of Arizona, Tucson

**Abstract.** Observations of reflected solar radiation measurements from natural surfaces (e.g., clouds and forested biomes) are often noted as disobeying the principle of reciprocity. In these contexts the application of reciprocity has been in its directional form. We note that the general principle of reciprocity also encompasses spatial attributes and reduces to a directional form only when the areas of illumination and measurement are the same. In either form a proper reciprocal set of reflected solar radiation measurements can never be obtained due to our inability to control the area illuminated by the Sun. This may appear as a breakdown in the directional reciprocity of the observations, which has serious implications for remote sensing. Using Monte Carlo radiative transfer simulations, we demonstrate that the magnitude of the apparent reciprocity breakdown depends on three factors: (1) measurement resolution, with larger deviations occurring for higher resolutions; (2) Sun-view geometry, with larger deviations occurring for larger Sun/view zenith angles and differences between Sun and view angles; and (3) the distribution of scatterers within and surrounding the measurement area, making the deviations depend on scene type.

## 1. Introduction

In its original form the Helmholtz principle of general reciprocity [*von Helmholtz*, 1859] is translated as:

> 'From point A, a unit quantity of light of a specific color, and polarized in a specific direction, $\alpha$, travels in such a beam direction that after a series of reflections and refractions a quantity $x$ finally arrives at point B, polarized in a direction $\beta$. If we now radiate the latter point (B) in the reverse direction of the final beam with a unit quantity of $\beta$-polarized light of the same color, there arrives after all those reciprocal and reversible processes the light has experienced, the same quantity $x$, therefore the same fraction, of $\alpha$-polarized light at the point of origin (A).'

Since it first appeared, the principle has become a fundamental principle in radiative transfer, and applies to absorbing and scattering media, with only a few exceptions (e.g., fluorescence). Note that the general principle of reciprocity has spatial, directional, and polarization attributes. The principle has been demonstrated to be equally valid for unpolarized light and with complete mathematical rigor [e.g., *Case*, 1957]. Many other physical systems have also been demonstrated to obey a reciprocity principle, and the principle has become a powerful mathematical tool in many branches of physics (see *Cook* [1996] for a review). In this study, the reciprocal behavior of reflected solar radiation measurements is examined. Emphasis is placed on measurements over clouds and other natural surfaces.

Recently, the application of reciprocity to reflected solar radiation measurements has been used to fill in missing data values in the generation of angular dependence models (ADMs) that describe the anisotropy of the upwelling radiation field over a particular scene type [e.g., *Kriebel*, 1996; *Suttles et al.*, 1988]. It has also been suggested that ADMs should be modified to obey reciprocity [e.g., *Green et al.*, 1990] or that the observations should be constrained to fit a particular reciprocal ADM [e.g., *Rahman et al.*, 1993]. In these contexts the application of reciprocity stems from its plane-parallel form [*Chandrasekhar*, 1960]:

$$\mu_0 \tilde{I}(\mu_0, \varphi_0; \mu, \varphi; \tau) F(\mu_0, \varphi_0) = \mu I(\mu, \varphi; \mu_0, \varphi_0; \tau) \tilde{F}(\mu, \varphi) \quad (1)$$

where $I(\mu, \varphi; \mu_0, \varphi_0; \tau)$ is the upward radiance in direction $(\mu, \varphi)$, $\mu$ being the cosine of the viewing zenith angle and $\varphi$ being the viewing azimuth angle caused by a downward solar irradiance $F(\mu_0, \varphi_0)$, $\mu_0$ being the cosine of the solar zenith angle, and $\varphi_0$ being the solar azimuth. Here $\tau$ is a variable that describes the scene type (e.g., for plane-parallel clouds, $\tau$ represents



Paper number 98JD00345.
0148-0227/98/98JD-00345$09.00

the optical depth) and is used to emphasize that the same scene needs to be observed during reciprocal measurements. The tilde symbol is used to emphasize that the observations of $I$ and $\tilde{I}$ are usually taken at different times. Equation (1) often appears written without $F$, where $F$ and $\tilde{F}$ are assumed to cancel each other out. When this form is used, the observed radiances may need to be corrected for variations in the Earth–Sun distance. However, other problems with temporal sampling may exist.

For example, the Earth Radiation Budget Experiment (ERBE) ADMs were derived from a statistical analysis of 205 days of ERB scanner measurements [*Suttles et al.*, 1988]. Equation (1) was used to fill in angular bins that were missing data. In such a statistical analysis, however, (1) can be applied correctly only when the spatial and temporal distribution of $\tau$ remain the same as we switch directions between cause and effect. Given that cloud properties possess a diurnal cycle [e.g., *Minnis and Harrison*, 1984; *Duvel*, 1989], it is unlikely that the same $\tau$ distribution is observed as we switch directions between cause and effect, especially when the difference between Sun and view angles is large. Thus, over many observations of a particular reciprocal set of directions, the appropriate application of the reciprocity principle is limited by our ability to classify the scene properly in terms of optical depth, at least as applied to plane-parallel clouds. The ERBE cloud classification (defined only by four cloud fractions) is too coarse to capture this aspect; however, we note that definite improvements in this regard will be made by the Clouds and the Earth Radiant Energy System (CERES) cloud classification strategy [*Wielicki et al.*, 1996].

*Davies* [1994] termed (1) the principle of directional reciprocity, since the general principle encompasses both spatial and directional attributes. He used ERBS data to show that directional reciprocity breaks down over scenes containing cloud. He further showed by example that the breakdown may be due to the horizontally heterogeneous nature of the cloud field. However, this example is not general, and examples of horizontally homogeneous scenes that violate directional reciprocity are also possible, depending on the illumination conditions (see section 2). As shown below, understanding the spatial relationship between illumination and measurement becomes a key factor in understanding the observed breakdown of directional reciprocity.

*Kriebel* [1996] has also observed that radiance measurements of natural Earth surfaces do not obey reciprocity. Since he was concerned with measurements taken near the Earth's surface, he examined the role of the diffuse sky radiation as a possible explanation for the nonreciprocal nature of the observed radiances. Even after correcting the diffuse sky radiation contribution, he was unable to explain why the solar reflectance measurements from the Earth's surface still appeared to be nonreciprocal.

While the basic difficulty in using directional reciprocity is simply due to horizontal spatial effects in illumination and measurement (section 2), these effects on the measurements vary with scene type and resolution, and require deeper examination. The remainder of this article explains why and how directional reciprocity breaks down. In particular, section 2 discusses the proper application of the general principle of reciprocity, the difficulties in applying it over clouds and other surfaces illuminated by the Sun, and the condition required to reduce it to a directional principle. In so doing, we introduce three propositions concerning the application of reciprocity in order to clarify the discussion. In section 3 these propositions are illustrated by examples from Monte Carlo simulations applied to heterogeneous cloud fields. The simulations reveal the behavior of directional reciprocity breakdown with regard to variables such as Sun/view geometry, scene type, and spatial resolution of the measurements. Of particular interest is the strong dependence of the breakdown on measurement resolution, implying that ADMs of natural surfaces should be resolution-dependent. Section 4 summarizes our results and addresses the implications for remote sensing.

## 2. Theoretical Background

The original form of the general principle of reciprocity (given at the beginning of section 1) and (1) lack the details needed for our application. *Case* [1957] has given a rigorous mathematical formulation of the general principle of reciprocity. However, interpretation is needed to understand how to apply the principle to remotely sensed measurements of reflected solar radiation. We therefore introduce three simple propositions concerning reciprocity that allow us to form a clear argument needed to explain the observed breakdown of directional reciprocity of reflected radiances from extended scenes.

Based on von Helmholtz's original form of reciprocity, it is unclear which measurement units should be assigned to the "unit quantity of light." This was clarified by *Minnaert* [1941] in a series of thought experiments. Figure 1 is based on one of these. Consider two small apertures, denoted by $A$ and $B$ with surface area $a$ and $b$, respectively, marking the only entry or exit points for an intervening medium which may scatter or absorb radiation. The areas are small enough that the radiance is constant over them. Let $f$ and $j$ be the incident and emerging radiances, respectively, and let $F$ and $J$ be the corresponding total intensities (i.e., the integral of the radiance over area, W $sr^{-1}$). Starting with an experiment in which $a = b$, both of unit area, we note $F = f$ at $A$ produces some amount $J = j$ at $B$.

For experiment 1, let $a = 2b$, so that $F = 2f$. This produces $2J = 2j$ at $B$. Experiment 2 is the reciprocal of experiment 1, in which $B$ is illuminated by $F = f$,

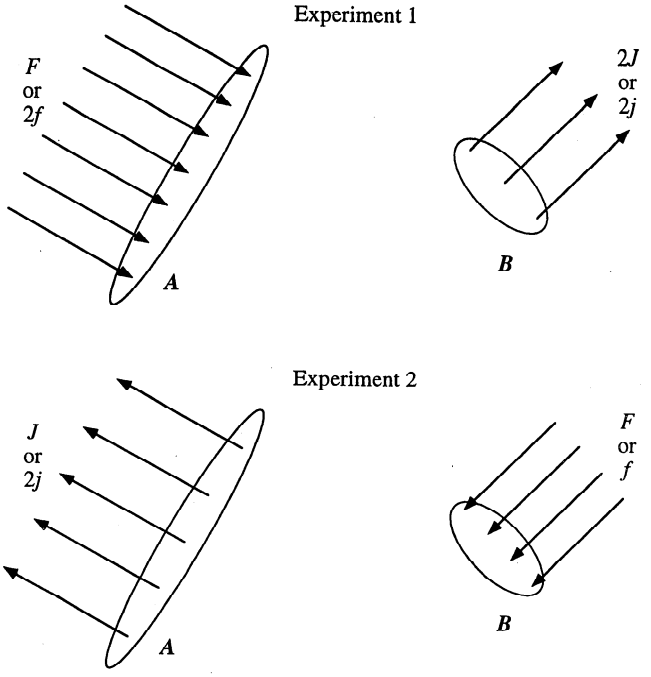


**Figure 1.** A reciprocal experiment depicting the general principle of reciprocity. $F$ and $J$ represent total intensities (W sr$^{-1}$), and $f$ and $j$ represent radiances (W m$^{-2}$ sr$^{-1}$). The areas of illumination or measurement are represented by surface elements $A$ and $B$. Reciprocity ensures that the total intensity emerging from surface area $B$ in experiment 1 is equal to the total intensity emerging from surface area $A$ in experiment 2, provided that the incident radiances are the same for both experiments. Alternatively, the radiance emerging from surface area $B$ in experiment 1 is equal to the radiance emerging from surface area $A$ in experiment 2, provided that the incident total intensities are the same for both experiments.

producing $J = 2j$ at $A$. Comparing these two experiments, we note that the measurement units should not be radiance to radiance, nor total intensity to total intensity, but rather radiance producing total intensity ($2f$ produces $2J$ in experiment 1, and $f$ produces $J$ in experiment 2), or total intensity producing radiance ($F$ produces $2j$ in both experiments). (Strictly speaking, this is true only if the indices of refraction at $A$ and $B$ are the same (as they are in the applications that we are considering); otherwise we need to account for the relative refractive index as shown by *Aronson* [1997]). We recommend reading *Minnaert* [1941] for additional examples of this nature, and summarize the general principle of reciprocity in modern terminology as proposition 1.

> **Proposition 1**: Let $A$ and $B$ represent two surfaces in space, and let the medium that fills the space be fixed in time during the reciprocal measurements. The general principle of reciprocity may be stated in the following way: the radiance emerging from $B$ in direction $\Theta_B$, caused by illuminating $A$ alone from direction $\Theta_A$ with total intensity $F$, is equal to the radiance emerging from $A$ in direction $\Theta_A$, caused by illuminating $B$ alone from direction $\Theta_B$ with total intensity $F$. The same holds for incident radiances and observed total intensities.

Although the use of radiance or total intensity is generally applicable, *Case* [1957] demonstrated that the irradiance (Wm$^{-2}$) can also be used when the scene is illuminated by parallel beams of radiation.

Consider the application of reciprocity when the illuminating source is the Sun and observations are made from a space-based radiometer. Due to the temporal variability of the media within a scene (e.g., clouds, aerosols, vegetation), the scattering and transmission properties of the scene may change between reciprocal measurements. For the moment we will assume there is no change. We will also assume that an identical area is viewed during the reciprocal measurement (e.g., no pixel expansion with viewing obliquity and perfect navigation). A problem still exists in observing reciprocity from satellite measurements because the Sun's illumination is almost always over the entire Earth's disc. A proper reciprocal pair of measurements (for given directions of $\Theta_A$ and $\Theta_B$ should consist of a measurement of the total intensity summed by the radiometer over $A$, caused by the Sun's illumination of the Earth's disc ($B$), and a measurement of the total intensity summed by the radiometer over the Earth's disc, caused by the Sun's illumination of $A$ alone. Although it may be possible to measure the total intensity over the Earth's disc, it is thus far impossible to have the Sun illuminate only a small subset of the Earth's disc. Therefore, in the application that we are considering, reciprocity cannot generally be observed for areas less than the entire Earth's disc since a proper reciprocal set of measurements cannot be obtained. For this reason, we adopt "apparent" reciprocity breakdown in our terminology.

There are cases, however, where directional reciprocity has been successfully applied to natural surfaces illuminated by the Sun; for example, in lunar photometry [e.g., *Minnaert*, 1941]. To better understand the successful application of directional reciprocity to these cases, we introduce the following proposition.

> **Proposition 2**: Let $\overline{A}$ be the complement of $A$ (i.e., $A \cap \overline{A} = \oslash$). If illuminating $\overline{A}$ causes no effect on measurements taken at $A$ for all illuminating angles, then the general principle of reciprocity can be applied to measurements taken at $A$ as if only $A$ were being illuminated.

The surface of the Moon satisfies the condition of proposition 2, since the radiance emerging from some lunar

region, $A$, is independent of whether $A$ alone or the entire lunar disc, $A \cup \overline{A}$, is being illuminated. However, the conditions for proposition 2 do not generally apply to solar radiation emerging from some region, $A$, at the top of the Earth's atmosphere, since there is generally a contribution to the radiance emerging from $A$ due to horizontal transport of solar radiation into $A$ from $\overline{A}$. This holds true for all surfaces that transport radiation horizontally (e.g., clouds and vegetation canopies). The magnitude of the contribution will depend on such factors as the size of $A$, the distribution of scatterers (e.g., liquid water in the case of clouds) within and surrounding $A$, and the Sun-view geometry. However, if this contribution of solar radiation is small relative to the radiance emerging from $A$, then the condition of proposition 2 is approximately satisfied and directional reciprocity should approximately hold true. For example, this may occur when the area of $A$ becomes large. Whether the scale of the ERBS field of view (FOV) is large enough for reciprocity to be applied to cloudy scenes is investigated in section 3; however, the results of *Davies* [1994] and *Loeb and Davies* [1997] suggest that it is not.

Finally, in plane-parallel theory, the general principle of reciprocity always reduces to a directional principle. However, we can be more encompassing.

> **Proposition 3:** The general principle of reciprocity always reduces to a directional principle when $A = B$.

In plane-parallel theory, the region over which cause and effect are defined is the same (i.e., a horizontally infinite domain); however, homogeneity of the scene is neither required (as mentioned earlier) nor sufficient for the application of directional reciprocity. This is in contrast to the statement made by *Loeb and Davies* [1997, p. 6878], that directional reciprocity "... requires the scene to be horizontally homogeneous over the pixel scale." For example, finite FOV measurements of scattered radiation from a horizontally infinite homogeneous cloud scene that is only partially illuminated will undergo an apparent reciprocity breakdown if the spatial attributes between illumination and measurement of propositions 1 or 3 are not observed. Thus, applying directional reciprocity to the example of a homogeneous scene found in the appendix of *Davies* [1994] is strictly correct only for the typical situation of complete illumination.

In the following section, aspects of the three propositions given above are demonstrated by way of Monte Carlo radiative transfer simulations through heterogeneous clouds. We demonstrate that the magnitude of the apparent reciprocity breakdown depends on the Sun-view geometry, the distribution of liquid water, and the resolution of the measurements.

## 3. Monte Carlo Simulations

In this section, Monte Carlo radiative transfer simulations through heterogeneous clouds are used to demonstrate several aspects of the propositions given in section 2. There are several advantages of using the Monte Carlo approach in this study: The accuracy of the simulated radiances can be increased by increasing the number of simulated photons; radiative transfer through realistic cloud fields can be simulated; the spatial resolution over which the simulated measurements are made can be varied; and the photon trajectories can be traced, thereby allowing us to determine the contributing sources to the simulated radiances. The disadvantage of using the Monte Carlo approach in this study is the vast amount of computational time required to obtain accurate radiances. As a result, it is impractical at this time to calculate, for example, the errors that have been introduced into the ERBE ADMs by using reciprocity in their derivation (to do so would also require complete knowledge of the distribution of cloud properties). Instead, we aim to demonstrate the correctness of the propositions given in section 2, to examine the variables that affect the magnitude of the apparent reciprocity breakdown, and to check if the conclusions drawn from the simulations coincide qualitatively with observations. This was accomplished through the analysis of many scenes; however, all scenes gave qualitatively similar results. We therefore give only one detailed example of a typical scene.

Figure 2 shows the cloud optical depth field used in this example. The field was derived from the advanced very high resolution radiometer (AVHRR; $\sim$ 1 km resolution) data using the method described by *Oreopoulos* [1996]. The scene is 256 pixels/side, has a cloud fraction $\approx$ 0.53, and a cloud-averaged optical depth $\approx$ 4.6. This field was used as input to the Monte Carlo radiative transfer model described by *Várnai* [1996]. The model assumes constant cloud base altitude and constant internal optical properties characteristic of water clouds. This gives rise to variable cloud top altitudes. It uses periodic boundary conditions, meaning that the cloud field is assumed to repeat infinitely in all directions beyond the initial 256 km region. To minimize possible effects of the boundary condition on the results, only areas that lie a distance of 10 km inward from the scene border are examined.

The Monte Carlo code calculates the upwelling radiance for solid angle bins, centered on each viewing direction, having an angular radius of 10°. To obtain exact correspondence between illumination and cloud reflection, the incident solar radiation reaching the cloud layer is assumed to isotropically fill a solid angle bin identical to that used for reflected radiances. Results are generated for seven solar and view directions, the centers of solid angle bins being at $\Theta = 0°$, 45°, and 75°, and $\varphi = 0°$, 90°, and 180°. It should be noted that for several reasons, such as the nonlinearity of the $\mu - \Theta$ relationship, the mean $\mu$ and $\mu_0$ values of these solid angle bins are not equal to the cosines of the central view angles. Instead, the effective $\mu$ and $\mu_0$ values are 0.992, 0.700, and 0.256. This results in 21 reciprocal pairs of radiance ratios that are not identically 1.

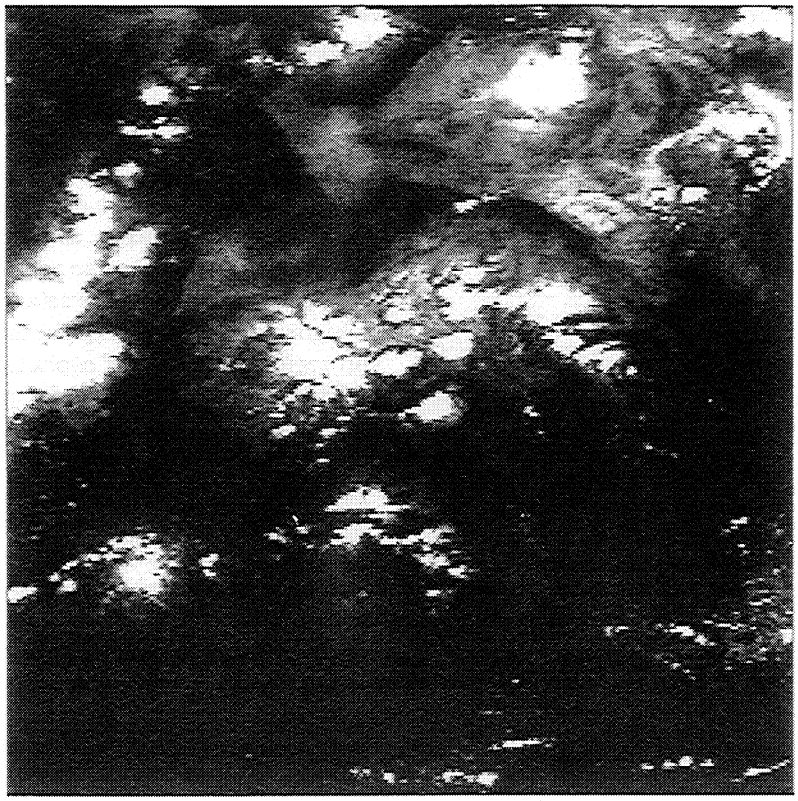

**Figure 2.** Cloud optical depth field used as input to the Monte Carlo example. The scene is 256 km on a side. The gray scale has been adjusted to enhance the cloud features.

The simulations assume conservative Mie scattering at 865 nm for the *Sctop* modified gamma drop size distribution of *Welch et al.* [1980]. Without loss of generality, the effects of the clear air and the underlying surface are ignored.

The Monte Carlo simulations were performed at the original resolution of the scene (1 km). The results were then spatially averaged to simulate coarser resolution measurements. Since the statistical uncertainty of the results increases with the resolution, no results are presented for resolutions higher than 10 km. Two sets of simulations were obtained in order to simulate nine measurement resolutions (equivalent to pixel FOV) ranging from 10 km to 236 km. For resolutions between 10 km and 40 km, our computational limitations did not allow us to obtain accurate results for the entire scene. Thus for such resolutions, only the 60 × 60 km$^2$ area centered in the scene depicted in Figure 2 was used. For resolutions between 40 km and 236 km, however, the entire 256 km × 256 km scene was used. Both experiments simulated the paths of the same number of photons (Table 1) through their respective cloud fields. The center portion contains similar features to the whole scene, and has a cloud average optical depth of 7.1. We will denote the whole scene in Figure 2 as region 1 and its 60 × 60 km$^2$ central portion as region 2. Simulated measurements were made at 10 km spacings for measurement resolutions $\geq$ 40 km, and 2 km spacings for measurement resolutions $\leq$ 40 km. Simulations at 40 km resolution were performed on both regions to examine discontinuities caused by the different regions. Using this strategy, the number of measurements and the number of simulated photons at each resolution for each region are shown in Table 1.

In our experiment it is useful to monitor two sets of photon trajectories: (1) $\alpha$-photons that both enter and exit the measurement area; and (2) $\beta$-photons that enter from outside the measurement area and exit within the measurement area. The sum of the two contributions ($\chi$-photons = $\alpha$-photons + $\beta$-photons) gives rise to the total measured radiance, thereby simulating what a radiometer would measure. In this way we can show that the $\alpha$-photons obey directional reciprocity, but the $\chi$-photons do not.

**Table 1.** Number of Measurements ($M$) and Simulated Photons ($N_t$) per Pixel at Each Resolution ($R$) for Each Region

| Region 1 | | | Region 2 | | |
|---|---|---|---|---|---|
| $R$, km | $M$ | $N_t(\times 10^6)$ | $R$, km | $M$ | $N_t(\times 10^6)$ |
| 40 | 400 | 7 | 10 | 256 | 7 |
| 60 | 324 | 16 | 15 | 169 | 16 |
| 100 | 196 | 44 | 20 | 121 | 28 |
| 160 | 64 | 113 | 30 | 36 | 63 |
| 236 | 1 | 246 | 40 | 1 | 112 |

In order to examine deviations from directional reciprocity, it is useful to define

$$\varepsilon = \frac{\mu_1 I(\mu_1, \varphi_1; \mu_2, \varphi_2; \tau)}{\mu_2 I(\mu_2, \varphi_2; \mu_1, \varphi_1; \tau)} - 1 \quad (2)$$

where the incident irradiances for the reciprocal experiment are the same and cancel. In Monte Carlo simulations, photon counts are measured. In terms of photon counts, (2) becomes

$$\varepsilon_\chi = \frac{\mu_2 \chi_1(\mu_1, \varphi_1; \mu_2, \varphi_2; \tau)}{\mu_1 \chi_2(\mu_2, \varphi_2; \mu_1, \varphi_1; \tau)} - 1 \quad (3)$$

where $\chi$ represents the number of $\chi$-photons measured (see *Várnai* [1996] to convert photon counts to radiances; here the photon counts are relative to the total incident number of photons, which are the same for all simulations, giving rise to the $\mu_1$ and $\mu_2$ terms in (3)). The parameters $\varepsilon_\alpha$ and $\varepsilon_\beta$ are defined in the same way. From proposition 3, $\varepsilon_\alpha = 0$. It is then easy to show that

$$\varepsilon_\chi = \frac{\beta_2}{\chi_2}\varepsilon_\beta \quad (4)$$

Equations (2)-(4) could also be defined with subscripts 1 and 2 interchanged. Note that as $\beta/\chi$ tends to 0, $\varepsilon_\chi$ also tends to zero. This happens when $\alpha \gg \beta$, which may occur when the measurement area becomes very large or when the conditions of proposition 2 are satisfied. But $\beta/\chi > 0$ is not a sufficient condition for $|\varepsilon_\chi| > 0$ (e.g., consider a plane-parallel homogeneous cloud illuminated everywhere with constant illumination); $|\varepsilon_\beta|$ also needs to be greater than zero. In the context of this study, such conditions occur when horizontal divergence of radiation exists over the areas that violate the spatial relationship of proposition 1 [see *Case*, 1957, equation (20)]. This occurs, for example, in media that are horizontally heterogeneous when the illumination is constant everywhere and measurements are made over a finite FOV.

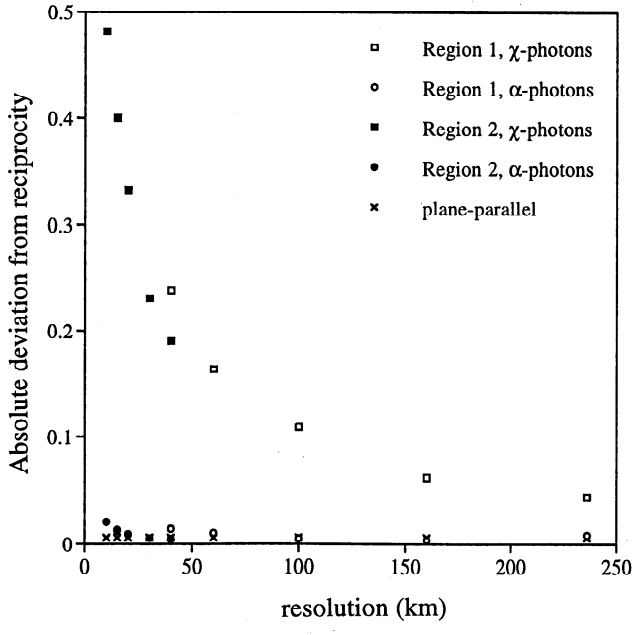


**Figure 3.** The absolute deviation of the reciprocal pair ratio from unity ($\varepsilon$), averaged over all reciprocal pair measurements, as a function of measurement resolution.

Figure 3 shows a graph of $|\varepsilon_\chi|$, averaged over all reciprocal pair measurements, as a function of measurement resolution. A value close to zero implies that directional reciprocity is obeyed. Five sets of data points are shown in Figure 3: one set of $\chi$-photons for each of region 1 and region 2, one set of $\alpha$-photons for each of region 1 and region 2, and one set for photons scattered from a plane-parallel scene having the same cloud-averaged optical depth as the clouds in region 2.

For simulations through the cloud fields of both regions 1 and 2, low photon numbers are observed in cloud-free and nearly cloud-free measurement areas. When the statistical uncertainty of the Monte Carlo simulations (see T. Várnai and R. Davies, A fast and accurate technique to simulate radiance fields reflected from 3-D cloud fields, submitted to *Applied Optics*, 1998) is greater than 5% for a given pixel, the measurement is rejected in all further analyses. For all points shown in Figure 3, the uncertainties are less than 2%, but vary from point to point.

The plane-parallel simulations obey reciprocity to within numerical uncertainty and are, of course, independent of resolution. They serve mainly to verify that the Monte Carlo code is behaving within numerical uncertainty caused by statistical fluctuations inherent to Monte Carlo procedures.

The $\alpha$-photons also obey reciprocity to within numerical uncertainty at all resolutions and are independent of the degree of inhomogeneity of the cloud field found within the measurement area. This is in accordance with proposition 3, given that measurements of $\alpha$-photons are equivalent to having the illuminated and measurement areas the same. The increase of numerical uncertainty at higher resolution is due to fewer photons being simulated per pixel (see Table 1).

The $\chi$-photon results shown in Figure 3 do not obey reciprocity at any of the measurement resolutions simulated. This is consistent with section 2, since simulations of the $\chi$-photons, which represent measurements of reflected solar radiation into a radiometer's FOV, do not obey the spatial relationship found in proposition 1, nor the conditions of proposition 2 for this example. Note that the $\chi$-photons undergo larger deviations from reciprocity as the measurement resolution increases. This is because the ratio of $\beta$-photons to $\alpha$-photons increases as the measurement resolution increases. Also note that the discontinuity at 40 km resolution is relatively small owing to the similarity of cloud distribution within regions 1 and 2.

Unfortunately, the literature reveals no published material on observed bidirectional reflection functions (BDRFs) of clouds that can be useful to assess the

resolution dependency of cloud ADMs. Much of what has been done for cloud ADMs has been derived from the Nimbus 7 ERB scanner [*Taylor and Stowe*, 1984]. The Nimbus 7 ADMs have since found application with other sensors, such as ERBE [*Suttles et al.*, 1988] and AVHRR [*Lubin et al.*, 1994]. However, if the magnitude of the reciprocity deviation is a function of measurement resolution, then so are ADMs (the proof is trivial). This implies that ADMs should be applied only to data of the same resolution as the data used to derive the ADMs. Figure 3 suggests that a cross-resolution application of ADMs becomes more inappropriate as the difference in resolution between the data used to derive the ADM and the data to which it is applied becomes larger. It also implies that ADMs derived by plane-parallel models, which are independent of resolution, are likely to be inappropriate for the real world. This implication is consistent with *Loeb and Davies* [1997], who find systematic differences between plane-parallel theory and observations. They also find that the ERBS measurements, at a degraded resolution of 160 km, deviate from reciprocity on average by about 5%. This 5% deviation is consistent with Figure 3, which represents our "typical" cloud scene.

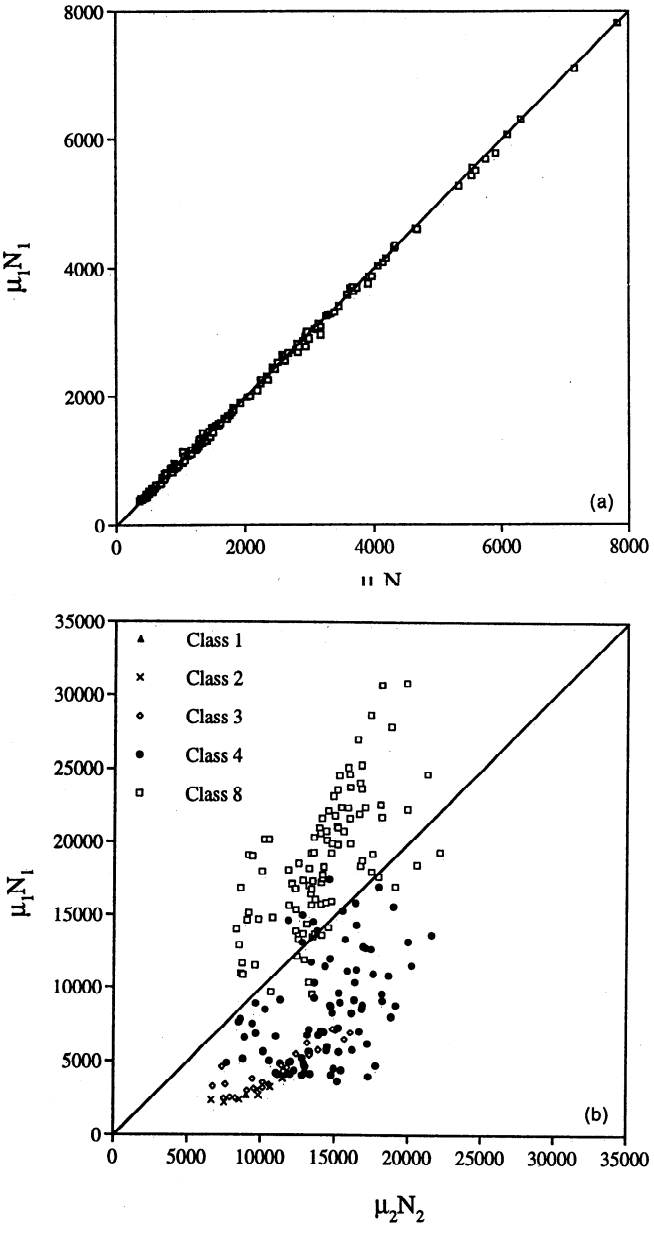


**Figure 4.** Scatterplots of the (75°, 0°; 45°; 90°) reciprocal pair at a measurement resolution of 10 km for (a) the $\alpha$-photons and (b) the $\chi$ photons. Photon counts, $N$, are used instead of radiances. $\mu_1 = 0.700$ and $\mu_2 = 0.256$. The scatter in Figure 4b is divided into scene types defined in Table 2. Note that only five of the eight scene types are present in the cloud field.

**Table 2.** Scene Type Classification Used in Figure 3b

| Class | Cloud Fraction, % | $\tau$ |
|---|---|---|
| 1 | $0 \leq CF < 25$ | $\tau \leq \tau_m$ |
| 2 | $25 \leq CF < 50$ | $\tau \leq \tau_m$ |
| 3 | $50 \leq CF < 75$ | $\tau \leq \tau_m$ |
| 4 | $75 \leq CF \leq 100$ | $\tau \leq \tau_m$ |
| 5 | $0 \leq CF < 25$ | $\tau > \tau_m$ |
| 6 | $25 \leq CF < 50$ | $\tau > \tau_m$ |
| 7 | $50 \leq CF < 75$ | $\tau > \tau_m$ |
| 8 | $75 \leq CF \leq 100$ | $\tau > \tau_m$ |

CF denotes cloud fraction; $\tau$ denotes optical depth; $\tau_m$ = 7.1 (mean cloud optical depth of region 2)

Figure 4 shows scatterplots of the (70°, 0°; 45°, 90°) reciprocal pair for the $\alpha$-photons and $\chi$-photons at a measurement resolution of 10 km. Points that lie along the diagonal obey reciprocity. The $\alpha$-photons clearly obey reciprocity to within statistical uncertainty; however, the $\chi$-photons do not. The scatter in Figure 4b is not random and depends on scene type. In this example, we define eight scene types by cloud fraction and optical depth as shown in Table 2. Note that the nonreciprocal nature of the radiances shows a systematic tendency that is a function of scene type. In fact, it not only depends on the distribution of liquid water within the pixel (as in our coarsely defined scene types), but also on that surrounding the pixel. Pixels containing low cloud fractions and optical depths tend to be affected by neighboring pixels that have large cloud fractions and optical depths; the converse is also true. As a result, the relative contribution of the $\beta$-photons to the $\chi$-photons, and hence the apparent reciprocity breakdown, can coarsely be broken down by scene type as demonstrated in Figure 4b. Similar conclusions can be drawn from all other reciprocal pairs at all other resolutions examined.

Our findings with regard to scene type cannot be tested against observed cloud BDRFs, for which there is an absence of useful data. However, some measured surface BDRFs exist that support our findings. The surface observations summarized by *Engelsen et al.* [1996] show that the deviations of the surface BRDFs from di-

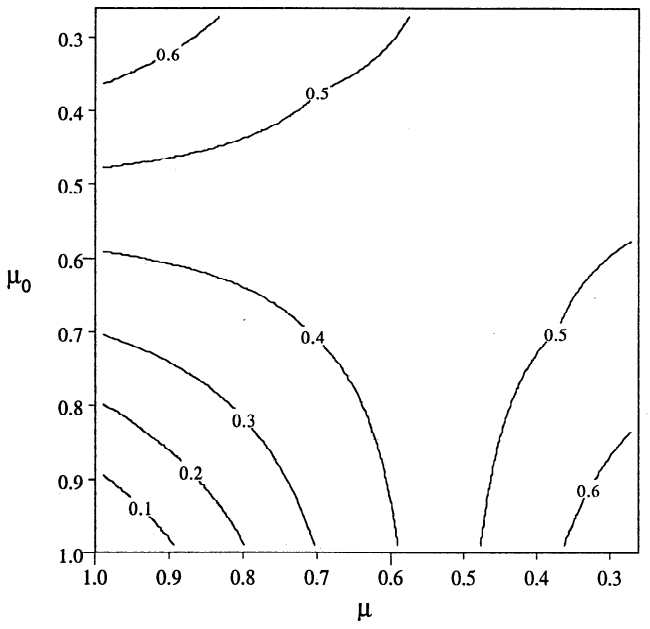


**Figure 5.** Values of $|\varepsilon_\chi|$ of the reciprocal pair $(\mu_1, \mu_2)$ for the 10 km resolution measurements averaged over azimuthal directions.

rectional reciprocity are a function of scene type, with a tendency for bare soils to be the most reciprocal and forested biomes the least. Bare soils tend to agree with proposition 2, whereas forested biomes can support horizontal transport of radiation. For forests the magnitude of the deviation from directional reciprocity will depend on the distribution of trees within and surrounding the measurement FOV.

Finally, Figure 5 shows a plot of $|\varepsilon_\chi|$ for 10 km resolution measurements averaged over azimuthal directions. We see that the magnitude of the deviation from reciprocity depends on the reciprocal angles. In general, the deviations increase with increasing Sun/view zenith angles and differences between Sun and view. This is because the relative contribution of $\beta$-photons to the total increases as the solar zenith angle becomes more oblique. Similar conclusions can be drawn from all other resolutions. The angular dependence of the apparent reciprocity breakdown is consistent with the observations of *Kriebel* [1996] and *Loeb and Davies* [1997]. Unfortunately, it is at large zenith angles where reciprocity is often most needed in constructing ADMs.

## 4. Summary and Conclusion

Observations of reflected solar radiation measurements from natural surfaces (e.g., clouds and forested biomes) are often noted as disobeying reciprocity [e.g., *Davies*, 1994; *Kriebel*, 1996; *Loeb and Davies*, 1997]. In these contexts the application of reciprocity has been in its directional form. The general principle of reciprocity given in proposition 1 encompasses spatial attributes as well and reduces to a directional form only when the areas of illumination and measurement are the same (cf. proposition 3). Given that the areas of illumination (the entire Earth's disc) and measurement (the radiometer's FOV) are generally not the same, directional reciprocity can be observed only under the special circumstances of proposition 2, or when the scene and its surrounding areas are sufficiently homogeneous. Moreover, a proper reciprocal set of measurements for general reciprocity cannot be obtained due to our inability to control the area covered by the illuminating source (i.e., the Sun always illuminates the entire Earth's disc). As a result the observations deviate from reciprocity because an unknown quantity of radiation enters from outside the instrument's FOV and contributes to the measured radiance. We have shown by way of Monte Carlo radiative transfer simulations that the degree to which the observations deviate from reciprocity will depend on three factors: (1) measurement resolution, with larger deviations occurring for higher resolutions; (2) Sun-view geometry, with larger deviations occurring for larger Sun/view zenith angles and differences between Sun and view; and (3) the distribution of scatterers within and surrounding the measurement area, making the deviations depend on scene type.

These findings have important implications for remote sensing techniques that use measurements of reflected solar radiation. The following are examples of such implications:

1. In certain cases the construction or retrieval of ADMs need not be constrained to obey directional reciprocity.

2. When using high or intermediate resolution measurements to derive ADMs and directional reciprocity to fill in missing directions, it is important to first combine enough measurements so that their total area is large enough for directional reciprocity to apply. This is especially important when directional reciprocity is used to fill missing ADM values for large viewing or solar zenith angles. Typically, directional reciprocity is expected to be always fulfilled to a sufficient degree at scales of several hundred kilometers for cloudy scenes, and at scales of several meters to kilometers for vegetated land and water surfaces.

3. Since the nonreciprocal behavior of the radiation field depends on measurement resolution, then so do ADMs in general. This implies that ADMs should be applied only to data of the same resolution as the data used to derive the ADMs. It also implies that ADMs derived by plane-parallel models or retrieval techniques based on the independent pixel approximation are likely to be inappropriate for the real world.

In addition to remote sensing, our findings also have implications for testing new radiative transfer calculation methods. In particular, one way to evaluate such methods is to examine whether the results obey the principle of reciprocity. If the method allows for controlled illumination, then the method can be tested using proposition 1. If the method allows for only directional reciprocity to be tested, then directional reci-

procity should be satisfied in either of the following conditions: proposition 2 is satisfied directly due to the nature of the scattering medium, the reflected radiances are averaged over the entire illuminated area (proposition 3), the scene is sufficiently homogeneous, or the reflected radiances are averaged over a sufficiently large region.

**Acknowledgments.** Partial support from the Jet Propulsion Laboratory of the California Institute of Technology under contract 959085 and from the Natural Sciences and Engineering Research Council of Canada are gratefully acknowledged. We also thank L. Oreopoulos for providing us with some interesting optical depth fields derived from AVHRR data, W. Decker for translating the original German form of von Helmholtz's theorem of reciprocity, and D. Flittner for useful suggestions toward the readability of the paper. We also appreciate the many interesting discussions on reciprocity with N. Loeb and R. Green. M. Sanderson-Rae edited the final manuscript and prepared it for publication.

## References

Aronson, R., Radiative transfer implies a modified reciprocity relation, *J. Opt. Soc. Am., A14*, 486–490, 1997.

Case, K. M., Transfer problems and the reciprocity principle, *Rev. Mod. Phys., 29*, 651–663, 1957.

Chandrasekhar, S., *Radiative Transfer*, sect. 52, pp. 171–177, Dover, New York, 1960.

Cook, R. K., Lord Rayleigh and reciprocity in physics, *J. Acoust. Soc. Am., 99*, 24–29, 1996.

Davies, R., Spatial autocorrelation of radiation measured by the Earth Radiation Budget Experiment: Scene inhomogeneity and reciprocity violation, *J. Geophys. Res., 99*, 20,879–20,887, 1994.

Duvel, J. P., Convection over tropical Africa and the Atlantic Ocean during northern summer, 1, Interannual and diurnal variations, *Mon. Weather Rev., 117*, 2782–2799, 1989.

Engelsen, O., B. Pinty, M. M. Verstraete, and J. V. Martonchik, Parametric bidirectional reflectance factor models: Evaluation, improvements and applications, *Rep. Eur. 16426*, 120 pp., Space Appl. Inst., Joint Res. Cent., Eur. Comm., 1996.

Green, R. N., J. T. Suttles, and B. A. Wielicki, Angular dependence models for radiance to flux conversion, *Proc. SPIE Int. Soc. Opt. Eng., 1299*, 102–111, 1990.

Kriebel, K.-T., On the limited validity of reciprocity in measured BRDFs, *Remote Sens. Environ., 58*, 52–62, 1996.

Loeb, N. G., and R. Davies, Angular dependence of observed reflectances: A comparison with plane parallel theory, *J. Geophys. Res., 102*, 6865–6881, 1997.

Lubin, D., P. Ricchiazzi, C. Gautier, and R. H. Whritner, A method for mapping Antarctic surface ultraviolet radiation using multispectral satellite imagery, in *Ultraviolet Radiation in Antarctica: Measurements and Biological Effects, Antartc. Res. Ser.*, vol. 62, edited by C. S. Weiler and P. A. Penhaler, pp. 53–81, AGU, Washington, D. C., 1994.

Minnaert, M., The reciprocity principle in lunar photometry, *Astrophys. J., 93*, 403–410, 1941.

Minnis, P., and E. F. Harrison, Diurnal variability of regional cloud and clear-sky radiative parameters derived from GOES data, II, November 1978 cloud distributions, *J. Clim. Appl. Meteorol., 23*, 1012–1031, 1984.

Oreopoulos, L., Plane parallel albedo bias from satellite measurements, Ph.D. thesis, McGill Univ., Montreal, Que., Canada, 1996.

Rahman, H., B. Pinty, and M. M. Verstraete, Coupled Surface-Atmosphere Reflectance (CSAR) model, 2, Semiempirical surface model usable with NOAA Advanced Very High Resolution Radiometer data, *J. Geophys. Res., 98*, 20,791–20,801, 1993.

Suttles, J. T., R. N. Green, P. Minnis, G. L. Smith, W. F. Staylor, B. A. Wielicki, I. J. Walker, D. F. Young, V. R. Taylor, and L. L. Stowe, Angular radiation models for the Earth-atmosphere system, vol. I, Shortwave radiation, *Rep. NASA RP-1184*, 147 pp., NASA, Washington, D. C., 1988.

Taylor, V. R., and L. L. Stowe, Reflectance characteristics of uniform Earth and cloud surfaces derived from Nimbus 7 ERB, *J. Geophys. Res., 89*, 4987–4996, 1984.

Várnai, T., Reflection of solar radiation by inhomogeneous clouds, Ph.D. thesis, McGill Univ., Montreal, Que., Canada, 1996.

von Helmholtz, H., Theorie der Luftschwingungen in Rohren mit offenen Enden, *Crelle, LVII*, 1, 1859.

Welch, R. M., S. K. Cox, and J. M. Davis, *Solar Radiation and Clouds, Meteorol. Monogr. Ser.* vol. 39, Amer. Meteorol. Soc., Boston, Mass., 1980.

Wielicki, B. A., B. R. Barkstrom, E. F. Harrison, R. B. Lee III, G. L. Smith, and J. E. Cooper, Clouds and the Earth Radiant Energy System (CERES): An Earth Observing System experiment, *Bull. Am. Meteorol. Soc., 77*, 853–868, 1996.

R. Davies, L. Di Girolamo, and T. Várnai, Institute of Atmospheric Physics, The University of Arizona, P. O. Box 210081, Tucson, AZ 85721-0081. (e-mail: larry@papagayo.atmo.arizona.edu)

(Received June 30, 1997; revised January 21, 1998; accepted January 26, 1998.)